Overlapping distribution of K_{ATP} channel-forming Kir6.2 subunit and the sulfonylurea receptor SUR1 in rodent brain

Christine Karschin[b], Claudia Ecke[a], Frances M. Ashcroft[c], Andreas Karschin[a,*]

[a]*Max Planck Institute for Biophysical Chemistry, Molecular Neurobiology of Signal Transduction, 37077 Göttingen, Germany*
[b]*Max Planck Institute for Experimental Medicine, 37077 Göttingen, Germany*
[c]*University Laboratory of Physiology, Parks Road, Oxford OX1 3PT, UK*

Received 18 September 1996; revised version received 20 November 1996

Abstract ATP-sensitive K^+ channels comprise a complex of at least two proteins: a member of the inwardly rectifying Kir6 family (e.g. Kir6.2) and a sulphonylurea receptor (e.g. SUR1) which belongs to the ATP-binding cassette (ABC) superfamily. Using specific radiolabeled antisense oligonucleotides, the cellular localization of both mRNAs was investigated in the rodent brain by in situ hybridization. The distribution of both transcripts was widespread throughout the brain and showed a high degree of overlap with peak expression levels in the hippocampus, neocortex, olfactory bulb, cerebellum, and several distinct nuclei of the midbrain and brainstem, indicating their important role in vital brain function.

Key words: K_{ATP} channel; Inward rectifier; Sulfonylurea receptor; In situ hybridization; ABC transporter

1. Introduction

ATP-sensitive potassium (K_{ATP}-) channels have been well defined both electrophysiologically and pharmacologically in cardiac, skeletal and smooth muscle, pancreatic β cells, pituitary, central and peripheral nervous system [1–5]. Their activity, and thus their various cellular functions, are controlled by the metabolism of the cell. It is generally believed that changes in ATP (which causes channel closure) and in MgADP (which activates the channel) couple metabolism to channel activity [6]. Differences in the macroscopic and single channel properties and in sensitivity to K^+ channel openers (which increase channel activity [7]) and sulphonylureas (which inhibit channel activity [8]), suggest that K_{ATP} channels comprise a molecularly heterogenous class of ion channels.

Recent findings demonstrate that functional K_{ATP} channels result from the molecular interaction between two proteins, one of which is an inwardly rectifying K^+ channel subunit (Kir6.2 or Kir6.1) and the other which is a high-affinity receptor for sulphonylureas (SUR1 or SUR2). The latter belongs to the ATP-binding cassette superfamily [9–12]. When heterologously expressed neither Kir6.2 nor SUR1/2 alone gave rise to channel activity, suggesting that neither of them is capable of forming functional K_{ATP} channels alone. Both K_{ATP} channel subunits may couple with related family members to form functional channels. For example, heterologously expressed Kir6.1 is also able to couple to SUR1, while SUR2, a related sulphonylurea receptor can couple to Kir6.2 to form a functional K_{ATP} channel. The similarity of the properties of the native β cell and neuronal K_{ATP} channels suggests they may be composed of the same subunits. The β cell K_{ATP} channel is formed from Kir6.2 and SUR1. This channel is important in regulating insulin secretion from pancreatic β cells and mutations in SUR1 result in hyperinsulinemic hypoglycemia of infancy, in which excess insulin secretion occurs [13].

In the brain, it is established that metabolic stress, such as hypoxia and/or glucose deficiency results in activation of K_{ATP} channels. Their precise functional role under physiological conditions, however, is still under debate. Northern blot analysis revealed only low levels in the brain of either Kir6.2 or SUR1, two prime candidates for K_{ATP} channel formation [10]. In this report, we demonstrate in detail their abundant and mostly overlapping mRNA localization at the cellular level using in-situ-hybridization histochemistry.

2. Materials and methods

In-situ hybridization analysis was performed on adult rat and mouse brain sections using 45–50 base pair synthetic antisense and sense oligonucleotides from regions in the untranslated region (UTR) or open reading frame (ORF) showing least similarity to other subfamily members (see below), to minimize cross-hybridization. The high specificity and effectiveness of the probes as well as their background labeling was tested as described before for Kir2.0 and Kir3.0 subfamily members [14]; controls used sense oligonucleotides in adjacent sections, RNAase digestion before hybridization, and hybridization with a mixed oligonucleotide probe containing a 10-fold excess of cold probe.

The sequence and location (base position on coding strand indicated) of the oligonucleotides used for data analysis were as follows: **Kir6.2** *3′ ORF antisense* ^{1301}5′GGACAAGGAATCCGGAGAGATGCTAAACTTGGGCTTGGCCTTTGC3′ (mouse with two mismatches to the rat ortholog; [10,11]), **Kir6.2** *3′ UTR* $^{+85}$5′GTCTGGCCAAGAGGCTCGCACCCCACCACTCTACATACCATACTT3′ (mouse with no specific match to the rat ortholog); **SUR1** *ORF antisense* ^{2164}5′AGCGAGGACTTGCCACAGCCCACCTGCCCCACGATCATGGTCAGC3′ [9]; **SUR1** *3′ ORF/UTR antisense* $^{+35}$5′GGTGAGGTGTGGGGTGGCACTTTGGCGCTGGCTGGTCATTTGTC. Oligonucleotides were 3′ end-labeled with [^{35}S]dATP (DuPont/New England Nuclear, 1200 Ci/mmol) by terminal deoxynucleotidyl transferase (TdT, Boehringer Mannheim, Germany) and used for hybridization at concentrations of 2–10 pg/μl (400 000 cpm/100 μl hybridization buffer per slide). For tissue preparation, adult Wistar rats and adult NMRI mice were anesthetized, decapitated and the brain removed and quickly frozen on dry ice. Brains were cut on a cryostat at 10–16 μm, thaw-mounted onto silane-coated slides, fixed with 4% paraformaldehyde in phosphate-buffered saline (pH 7.4), dehydrated and stored under ethanol until hybridization. Slides were airdried and hybridized overnight at 43°C in 100 μl buffer containing 50% formamide, 10% dextran sulfate, 50 mM DTT, 0.3 M NaCl, 30 mM Tris-HCl, 4 mM EDTA, 1×Denhardt's solution, 0.5 mg/ml denatured salmon sperm DNA, and 0.5 mg/ml polyadenylic acid. Sections were washed 2×30 min in 1×SSC plus 50 mM β-mercaptoethanol, 1 h in 1×SSC at 60°C, and 10 min in 0.1×SSC at room temperature. Specimens were then dehydrated, air-dried and exposed to Kodak Biomax X-ray film for 8–34 days. For cellular

*Corresponding author. Fax. (49) (551) 201 1688,
E-mail: AKARSCH@GWDG.DE

PII S0014-5793(96)01438-X

resolution, selected slides were subsequently dipped in photographic emulsion Kodak NTB2, incubated for 8–16 weeks and then developed in Kodak D-19 for 2.5 min. For analysis with bright- and dark-field optics, sections were Nissl counterstained with cresyl violet to confirm cytoarchitecture. Brain structures were identified and confirmed according to Paxinos and Watson [15].

3. Results

Analysis of the widespread mRNA expression in the mouse brain (Kir6.2/SUR1) and rat brain (SUR1) was performed on X-ray film images and emulsion-dipped parasagittal, coronal, and horizontal sections and is summarized in Table 1. Both antisense oligonucleotide probes specific for a given subunit mRNA revealed identical labeling profiles in a given species, demonstrating the specificity and effectiveness of the hybridi-

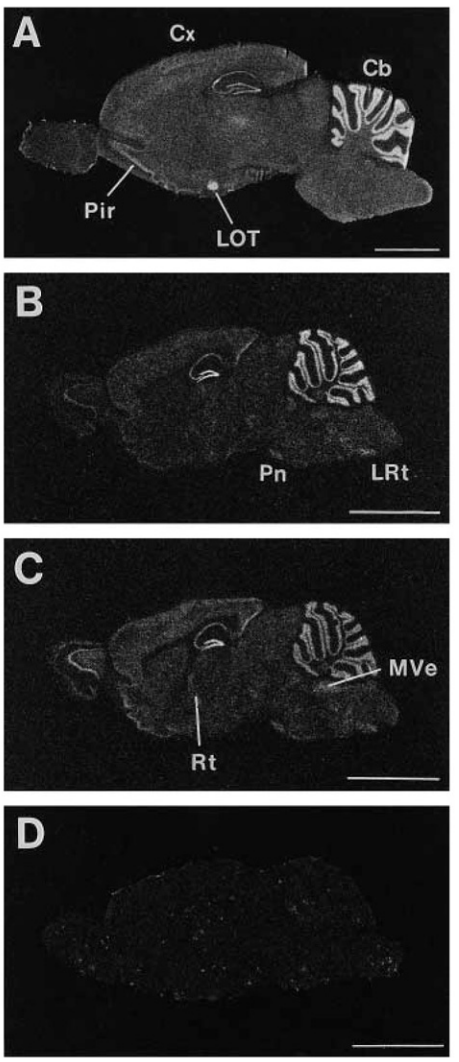

Fig. 1. X-ray film images of rat brain (A) and mouse brain (B–D) sagittal sections showing the distribution of SUR1 (A,B) and Kir6.2 mRNA (C) transcripts as revealed by in situ hybridization with specific oligonucleotide probes. (D) Control section digested with RNases before hybridization to Kir6.2 antisense probe. Slides were exposed to X-ray film for 17 days (A), 21 days (B,C), and 34 days (control). Bright areas indicate high expression levels. Cb, cerebellum; Cx, neocortex; LOT, nucleus of the lateral olfactory tract; LRt, lateral reticular nucleus; MVe, medial vestibular nucleus; Pn, pontine nucleus; Pir, piriform (olfactory) cortex; Rt, thalamic reticular nucleus. Scale bars represent 400 μm.

Table 1
Distribution of Kir 6.2/SUR1 mRNAs in the adult mouse and rat brain

Brain region	Kir6.2	SUR1
Olfactory bulb		
Granule cells	+	+
Mitral cells	+++	++
Periglomerular cells	++	++
Anterior olfactory nucleus	++	+++
Olfactory tubercle	++	++
Piriform cortex	+++	+++
Neocortex	+++	+++
Subiculum	++	+++
Entorhinal cortex	+++	+++
Hippocampus		
Dentate gyrus granule cells	+++	+++
CA1, CA3 pyramidal cells	++	++
CA2 pyramidal cells	++	++++
Tenia tecta	+++	+++
Indusium griseum	+++	+++
Septum		
Bed nuclei of stria terminalis	+	+
Lateral septal nucleus	+	+
Septohippocampal nucleus	+	++
Nuclei of the diagonal band	+++	++
Basal ganglia		
Caudate putamen	++	+
Globus pallidus	++	+
Ventral pallidum	+	+
Nucleus accumbens	++	0
Subthalamic nucleus	+++	+
Substantia nigra	++	++
Zona incerta	++	+
Amygdala	+	+
Lateral olfactory tract nucleus	+++	++++
Hypothalamus	+	+
Preoptic area	+	+
Magnocellular preoptic nucleus	+++	nd
Thalamus		
Thalamic reticular nucleus	++	+
Geniculate nuclei	+	+
Anterior dorsal nucleus	+++	++
Lateral nuclei	+	+
Ventroposterior nuclei	++	++
Midbrain		
Superior colliculus	++	+
Inferior colliculus	++	++
Central gray	++	nd
Red nucleus	++	++
Oculomotor nucleus	++	+
Ventral tegmental area	++	+
Lateral lemniscus nuclei	++	+
Cerebellum		
Deep nuclei	+++	++
Molecular layer	+	+
Granule cell layer	+	++
Purkinje cells	+++	+
Brainstem		
Pontine nucleus	++	+++
Inferior olivary nuclei	+	0
Locus coeruleus	+	nd
Raphe nuclei	+	+
Pontine reticular formation	++	++
Spinal trigeminal nucleus	++	++
Facial nucleus	+	+++
Vestibular nucleus	+++	++
Cochlear nuclei	+++	++
Hypoglossal nucleus	+++	++
Lateral reticular nuclei	+++	+++

For analysis of emulsion-dipped slides, silver grain density over the most intensely labeled cell bodies was rated as very strong (++++), and other brain regions were rated in relation to this maximal signal as strong (+++), moderate (++), low (+), or background level (0); (nd) expression could not be determined. Kir6.2 mRNA expression was determined in mouse brain and SUR1 in rat brain sections.

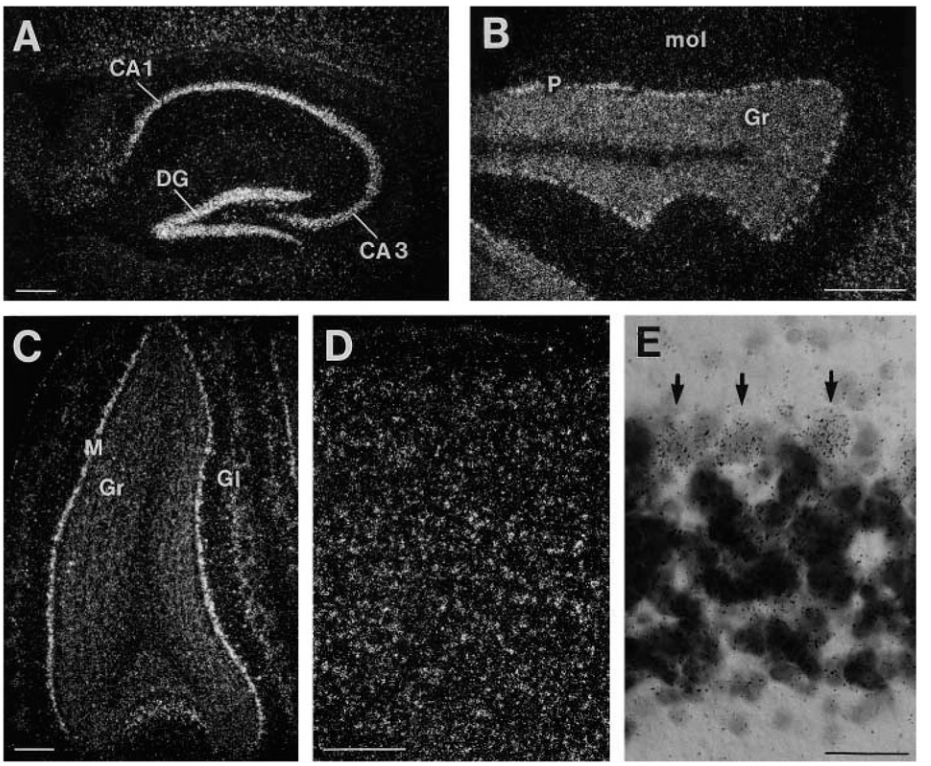

Fig. 2. Dark-field photomicrographs of Kir6.2 mRNA expression in adult mouse brain. (A) In hippocampus, strongest expression is seen in dentate gyrus granule cells; (B) cerebellum; (C) main olfactory bulb; (D) cortex; (E) bright field view of cerebellum; arrowheads point to Purkinje cells (P). CA1–CA3, pyramidal cell layers of hippocampus; DG, dentate gyrus; Gl, glomerular cells; Gr, granule cell layers; M, mitral cells; mol, molecular layer. Scale bars represent 250 μm (A–D), 30 μm (E).

zation probes. Only background labeling was observed when adjacent sections were hybridized with a sense strand probe or when the tissue was digested with RNases before hybridization (Fig. 1D). In general, the expression patterns of Kir6.2 and SUR1 mRNAs were widely overlapping and pronounced hybridization signals were observed for both mRNAs in the majority of brain regions. Compared to the expression patterns of other Kir subfamily members [14], the expression of both transcripts was more widespread and diffuse (Fig. 1) and was thus more difficult to analyze. Several brain regions with prominent differences in labeling intensities are discussed in detail below.

3.1. *Kir6.2 mRNA*

In the olfactory system most intense labeling was detected in the mitral cells of the olfactory bulb, whereas granule cells displayed only a weak hybridization signal (Fig. 2C). Moderate expression was also seen in the glomerular cells, in the anterior olfactory nucleus and in the olfactory tubercle. Kir6.2 mRNA was particularly elevated in the nucleus of the lateral olfactory tract (LOT), a conspicuous cortical-like nucleus at the rostromedial pole of the amygdala. The amygdala proper was only weakly labeled, as were the hypothalamus and most parts of the preoptic region except the strongly labeled magnocellular preoptic nucleus. In the cortex, large neurons were strongly labeled in all layers of the neocortex (Fig. 2D), as well as the piriform, entorhinal and subicular cortex. In hippocampus, Kir 6.2 subunit mRNA expression was strongest in dentate gyrus granule cells and in CA1–CA3 field pyramidal cells (Fig. 2A). In the basal ganglia we observed only moderate levels of Kir6.2 mRNA expression in the caudate putamen, globus pallidus, ventral pallidum, nucleus accumbens and in the substantia nigra, a site of prominent [^{3}H]glibenclamide binding. Only the subthalamic nucleus which provides the major excitatory input to the substantia nigra showed elevated Kir6.2 expression levels. In the septum, the nuclei of the diagonal band contained high levels of Kir6.2 transcript; surprisingly, the septohippocampal nucleus, which displays moderate levels of SUR1 mRNA (Fig. 3C) and a high sulphonylurea receptor density as assessed by [^{3}H]glibenclamide autoradiography [24], showed only low levels of Kir6.2 mRNA.

In the thalamus, the hybridization signal was weak or moderate in most nuclei, except for the reticular nucleus (Fig. 1C) and the small anterodorsal nucleus, which was among the most strongly labeled brain structures. In the midbrain we observed a generally moderate expression level with slightly higher levels in the inferior colliculus, the lateral lemniscus, the red and oculomotor nucleus compared to the superior colliculus and the central gray matter. In the cerebellum all large neurons in the deep nuclei were strongly labeled. All Purkinje cells in the cerebellar cortex were strongly positive, whereas cells in the granular and molecular layers displayed only weak hybridization signals (Fig. 2B,E). In the lower brainstem, Kir6.2 mRNA was expressed by neurons in the reticular fields as well as in distinct nuclei, with highest levels in vestibular, cochlear, hypoglossal, trigeminal, and lateral reticular nuclei. Very low labeling or only background levels were observed in the facial nucleus and the inferior olive, respectively.

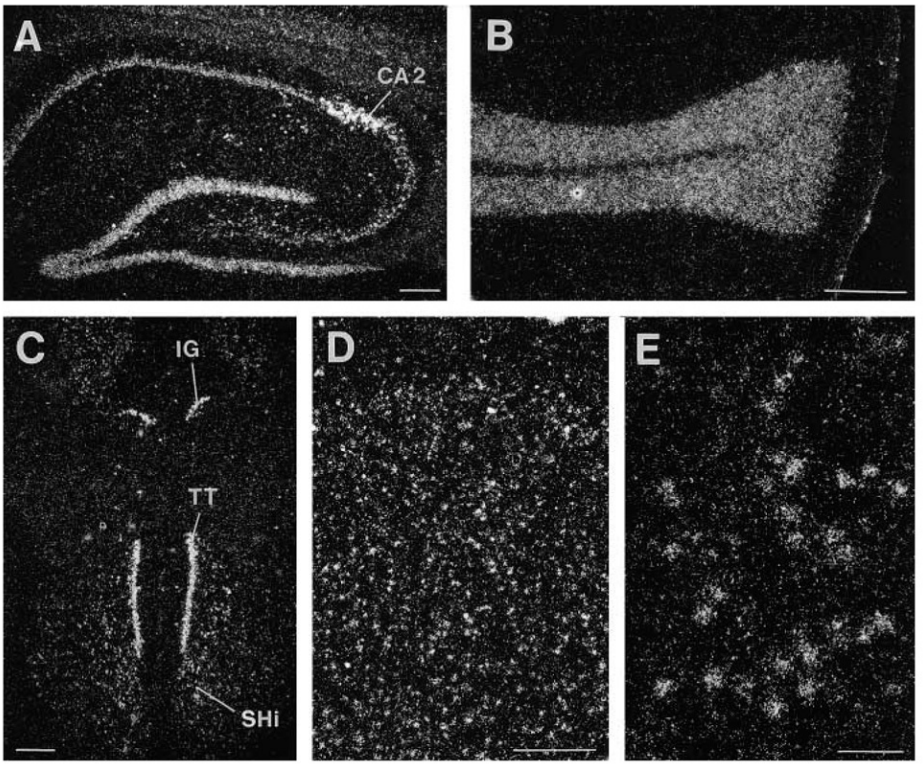

Fig. 3. Dark-field photomicrographs of SUR1 mRNA expression in adult rat brain. (A) Hippocampus; (B) cerebellum; (C) tenia tecta and adjacent septal nuclei; (D) cortex; (E) brainstem facial nucleus. CA2, pyramidal cell layer of hippocampus; IG, indusium griseum; SHi, septohippocampal nucleus; TT, tenia tecta. Scale bars represent 250 μm (A–D), 100 μm (E).

3.2. SUR1 mRNA

These transcripts were also widely expressed throughout the brain (see Table 1) with basically identical distribution patterns in rat and mouse. Two populations of neurons with exceptionally strong expression stand out: the hippocampal CA2 pyramidal cells (Figs. 1A and 3A) and the LOT neurons at the cortical amygdala, both of these areas also strongly express Kir6.2 mRNA. High SUR1 levels were found in all layers of neocortex (Fig. 3D), piriform cortex (Fig. 1A), hippocampus dentate gyrus granule cells (Fig. 3A), tenia tecta, indusium griseum (Fig. 3C), anterior olfactory nucleus, and most of the lower brainstem nuclei (Fig. 3E). These areas displayed high levels of Kir6.2 mRNA as well. Analysis of specific nuclei containing large, loosely grouped neurons (e.g. brainstem lateral reticular, pontine or vestibular nuclei) revealed that most of these neurons were labeled when hybridized to either Kir6.2 or SUR1 specific probes, suggesting colocalization of the two mRNAs. SUR1 mRNA levels were moderate to low in the olfactory bulb, throughout the thalamus and midbrain and in the septal nuclei with a more pronounced expression in the septohippocampal nucleus (Fig. 3C). Low levels were found in the amygdala, hypothalamus, preoptic region and also in the basal ganglia where prominent [^{3}H]glibenclamide staining suggests high SUR density; only the substantia nigra displayed moderate labeling. In the cerebellum large neurons in the deep nuclei were labeled as observed with Kir6.2 specific probes; Purkinje cells were positive, but less strongly labeled compared to Kir6.2 mRNA..

Two areas with elevated expression levels, where Kir6.2 mRNA expression was weak, were the dorsal endopiriform nucleus and the claustrum. Conversely, SUR1 transcripts were low in nuclei such as the subthalamic, oculomotor and lateral lemniscus nuclei, where a pronounced Kir6.2 expression was observed.

Compared to Kir6.2 specific probes a higher silvergrain density was observed with all oligoprobes specific for SUR1 over white matter fiber tracts. Silvergrains, however, did not significantly accumulate over oligodendrocyte cell bodies which is in agreement with the negative [^{3}H]glibenclamide binding in rat brain fiber tracts [24].

4. Discussion

In this report we describe the cellular localization of two mRNA transcripts that may be expected to form ATP-sensitive K^+ channels in the rodent brain. There is evidence that the K_{ATP} channel in pancreatic β cells is formed from a complex of Kir6.2 and SUR1 subunits. K_{ATP} channels (type I) with similar properties have been described in various neurons, including those of the cerebral cortex, substantia nigra, caudate and hippocampus (e.g. [16,17]). Like the β cell K_{ATP} channels, they have single channel conductances between 60 and 75 pS, are inhibited by sulphonylureas and activated by the K^+ channel opener diazoxide. These brain regions also express mRNA transcripts for Kir6.2 and SUR1, suggesting that a complex of these two proteins may also form a brain K_{ATP} channel. An additional type of K_{ATP} channel (type II) with much lower, millimolar ATP sensitivity, a larger unitary conductance (150 pS) and a different pharmacology, has been described in neurons of the ventromedial hypothalamic nucleus. These channels may play a role in the glucose-sensing mechanism involved in appetite control [18]. Their very dif-

ferent biophysical and pharmacological properties argue that they may be formed from proteins different to type I K_{ATP} channels.

Combining physiological data and mRNA distribution patterns, the prime question remains as to whether the molecular composition of native K_{ATP} channels in a given neuron can eventually be deciphered. Under the assumption that K_{ATP} channels comprise a complex between Kir channel and SUR subunits, functional diversity may arise from different combinations of possibly several isoforms of either component. Ämmälä et al. [19] recently described promiscuous coupling between recombinant SUR1 and Kir1.1, Kir6.1 and Kir 6.2, yielding Ba^{2+}- and tolbutamide-sensitive K^+ inward currents. In contrast, SUR1 interactions with other Kir subfamily members, e.g. Kir2.0 or Kir3.0, have never been reported. As mentioned in a previous study, we did not detect significant levels of Kir1.1 (ROMK1) transcripts in the brain [20], but rather in the outer medulla of the rat kidney, suggesting an insignificant role in native brain K_{ATP} channels. In contrast, we found the ubiquitous Kir6.1 (uK_{ATP}-1; [21]), of which moderate mRNA levels in the brain were detected in the original Northern blots, in a distinct cell population throughout the brain using several different oligonucleotide probes (C. Ecke, unpublished observation). Positive cells had very small somata (< 7 μm in diameter) and were sparsely distributed; they may represent either glia or small interneurons, but further characterization will be necessary. Since SUR1 mRNA is predominantly expressed in large and medium-sized neurons, coexpression with Kir6.1 mRNA is highly unlikely.

While this manuscript was in preparation, Inagaki et al. [22] reported the cloning and functional characterization of a second SUR isoform with 68% amino acid identity to SUR1. Northern blot analysis localized SUR2 mRNA predominantly in the ovary, heart and skeletal muscle, but also at moderate levels in the brain. SUR2 when heterologously expressed together with Kir6.2 gives rise to type I K_{ATP} channels which had a unitary conductance of 79 pS, but were much less sensitive to ATP ($\sim$10-fold), glibenclamide ($\sim$500-fold), and the K^+ channel openers pinacidil and diaxozide than the pancreatic Kir6.2/SUR1 channel. In general, SUR2/Kir6.2 channels exhibit pharmacological features characteristic of K_{ATP} channels found in native cardiac and skeletal muscle [1,23]. Cross-hybridization with SUR2 transcripts under the hybridization conditions used in our experiments was highly unlikely for the 3′UTR SUR1 oligonucleotide (no specific sequence similarity to SUR2), and possible for the ORF probe (7 mismatches to SUR2). Probe specificity was also evident when employed on brain tissue of different species: the 3′UTR oligonucleotide only hybridized with rat, but not with mouse tissue, whereas the ORF probe gave identical results in both species. Since both probes revealed basically identical hybridization patterns in the mouse we conclude that they specifically recognize SUR1 transcripts. Using 5′ and 3′ antisense oligonucleotides specific for SUR2 ORF we have been unable so far to detect specific SUR2 mRNA labeling in the rat brain. In summary, all these findings suggest that neither SUR2 nor any Kir channel subunit other than Kir6.2 are likely to play a major role in type I K_{ATP} channels in the rodent brain; thus, as the most relevant candidates we have selected to investigate in detail the cellular localization of SUR1 andKir6.2 subunits.

Sulfonylurea receptors in the mouse and rat CNS have been localized before by autoradiography using [^{3}H]glibenclamide, which binds to a single class of sulphonylurea binding sites [24,25]. Since SUR1 has a much higher affinity to glibenclamide ($K_D \sim 1$ nM), most binding sites might reflect SUR1 rather than SUR2 which has a much lower affinity ($K_D \sim 1$ M). Consistently, highest densities of [^{3}H]glibenclamide binding sites were found in substantia nigra, globus pallidus, septohippocampal nucleus, neocortex, hippocampus and cerebellar molecular layer. We find Kir6.2 and SUR1 mRNA in all these regions with highest levels in hippocampus and cortex, but reduced levels in the other regions. Most strikingly, several sites with apparently few or non-existent [^{3}H]glibenclamide binding sites, revealed exceptionally strong hybridization signals for both Kir6.2 and SUR1 mRNAs (LOT, olfactory bulb mitral cells, deep cerebellar nuclei, vestibular, hypoglossal and spinal trigeminal brainstem nuclei, and neurons in the reticular formation). Naturally, mRNA expression levels may somewhat diverge from the actual amount of expressed channel/receptor protein present in a cell. Also, [^{3}H]glibenclamide binding may include the distribution of the protein on axon and dendrites, whereas mRNA levels reflect the expression of the message in the cell. In the cerebellum, the highest glibenclamide binding was found in the molecular layer, whereas SUR1 and Kir6.2 mRNA transcripts are found in the granule cell layer. Closer inspection, however, reveals that the highest receptor binding densities are found on the presynaptic (parallel) fibres of the granule cells. Both binding and mRNA studies therefore agree that the K_{ATP} channels are localized on the granule cell presynaptic terminals in the molecular layer. A similar explanation may be applied to the hippocampus, where neuronal somata and dendrites are spatially segregated and [^{3}H]glibenclamide binding in the stratum lucidum is located presynaptically on granule cell mossy fibers [25].

Furthermore, the pattern of [^{3}H]glibenclamide binding sites may comprise the gene products of SUR1, SUR2 or yet another receptor isoform with similar ligand binding characteristics that may or may not participate in neuronal K_{ATP} channel formation. The gross agreement in distribution patterns, however, of [^{3}H]glibenclamide binding, SUR1 mRNA and Kir6.2 mRNA, as well as mRNA colocalization in all large neurons of several brain nuclei supports the notion that SUR1/Kir6.2 translate to interact in the formation of a major class of K_{ATP} channels in the rodent brain.

Acknowledgements: We wish to thank R. Schubert for excellent technical assistance and Prof. W. Stühmer for his generous support. This study was supported in part by grants from the Deutsche Forschungsgemeinschaft.

References

[1] Noma, A. (1983) Nature 305, 147–148.
[2] Cook, D.L. and Hales, C.N. (1984) Nature 311, 271–273
[3] Spruce, A.E., Standen, N.B. and Stanfield, P.R. (1985) Nature 316, 736–738.
[4] Nicholas, B., Quayle, J.M., Davis, N.W., Brayden, J.E., Huang, Y. and Nelson, M.T. (1989) Science 245, 177–180.
[5] Ashford, M.L.J., Sturgess, N.C., Trout, N.J., Gardner, N.J. and Hales, C.N. (1988) Pflügers Arch. 412, 297–304.
[6] Ashcroft, S.J.H. and Ashcroft, F.M. (1990) Cell. Signalling 2, 197–214.
[7] Edwards, G. and Weston, A.H. (1993) Annu. Rev. Pharmacol. Toxicol. 33, 597–637.

[8] Ashcroft, F.M. and Ashcroft, S.J.H. (1992) Biochem. Biophys. Acta 1175, 45–59.
[9] Aguilar-Bryan, L., Nichols, C.G., Wechsler, S.W., Clement IV, J.P., Boyd III, A.E., González, G., Herrera-Sosa, H., Nguy, K., Bryan, J. and Nelson, D.A. (1995) Science 268, 423–426.
[10] Inagaki, N., Gonoi, T., Clement IV, J.P., Namba, N., Inazawa, J., González, G., Aguilar-Bryan, L., Seino, S. and Bryan, J. (1995) Science 270, 1166–1170.
[11] Sakura, H., Ämmälä, C., Smith, P.A., Gribble, F.M. and Ashcroft, F.M. (1995) FEBS Lett. 377, 338–244.
[12] Tokujama, Y., Fan, Z., Furuta, H., Makielsi, J.C., Polonsky, K.S., Bell, G.I. and Yano, H. (1996) Biochem. Biophys. Res. Commun. 220, 532.538.
[13] Thomas, P.M., Cote, G.J., Wohllk, N., Haddad, B., Mathew, P.M., Rabl, W., Aguilar-Bryan, L., Gagel, R.F. and Bryan, J. (1995) Science 268, 426–429.
[14] Karschin, C., Dissmann, E., Stühmer, W. and Karschin, A. (1996) J. Neurosci. 16, 3559–3570.
[15] Paxinos, G. and Watson, C. (1986) The Rat Brain in Stereotaxic Coordinates, Academic Press, Sydney.
[16] Schwanstecher, C. and Panten, U. (1994) Pflügers Arch. 427, 187–189.
[17] Ohno-Shosaku, T. and Yamamoto, C. (1992) Pflügers Arch. 422, 260–266.
[18] Ashford, M.L.J., Boden, P.R. and Treherne, J.M. (1990) Pflügers Arch. 415, 479–483
[19] Ämmälä, C., Moorhouse, A., Gribble, F., Ashfield, R., Proks, P., Smith, P.A., Sakura, H., Coles, B., Ashcroft, S.J.H. and Ashcroft, F.M. (1996) Nature 379, 545–548.
[20] Karschin, C., Schreibmayer, W., Dascal, N., Lester, H.A., Davidson, N. and Karschin, A. (1994) FEBS Lett. 348, 139–144.
[21] Inagaki, N., Tsuura, Y., Namba, N., Masuda, K., Gonoi, T., Horie, M., Seino, Y., Mizuta, M. and Seino, S. (1995) J. Biol. Chem. 270, 5691–5694.
[22] Inagaki, N., Gonoi, T., Clement IV, J.P., Wang, C.Z., Aguilar-Bryan, L., Bryan, J. and Seino, S. (1996) Neuron 16, 1011–1017.
[23] Davies, N.W., Standen, N.B. and Stanfield, P.R. (1991) J. Bioenerg. Biomembr. 23, 509–535.
[24] Mourre, C., Widmann, C. and Lazdunski, M. (1990) Brain Res. 519, 29–43.
[25] Tremblay, E., Zini, S. and Ben-Ari, Y. (1991) Neurosci. Lett. 127, 21–24.